

Supporting Information

Mn(II) Metal-Organic Frameworks Based on Mn₃ Clusters: From 2D Layer to 3D Framework by the “Pillaring” Approach

Yong-Qiang Chen, Sui-Jun Liu, Yun-Wu Li, Guo-Rong Li, Kun-Huan He, Ze Chang* and Xian-He Bu

Department of Chemistry, Tianjin Key Lab on Metal and Molecule-based Material Chemistry, Nankai University, Tianjin 300071, China

* Corresponding author. E-mail: changze@nankai.edu.cn. Fax: +86-22-23498361.

Table S1. Selected bond distances (\AA) and angles ($^\circ$) for complexes **1** and **2**

1			
Mn(1)–O(1)	2.222(3)	Mn(2)–O(1)	2.274(3)
Mn(2)–O(2)	2.252(3)	Mn(1)#1–O(3)	2.102(3)
Mn(2)#1–O(4)	2.061(3)	Mn(2)#2–O(5)	2.195(3)
Mn(2)#2–O(6)	2.308(3)	Mn(1)–O(7)	2.197(4)
Mn(2)–O(11)	2.193(4)	Mn(1)–O(7)#5	2.197(4)
Mn(1)–O(3)#4	2.102(4)	Mn(1)–O(3)#5	2.102(4)
Mn(1)–O(1)#5	2.222(3)	Mn(2)–O(4)#3	2.061(3)
Mn(2)–O(5)#6	2.195(3)	Mn(2)–O(6)#6	2.308(3)
Mn(1)–O(1)–Mn(2)	112.06(13)	O(7)–Mn(1)–O(3)#4	92.63(17)
O(7)#3–Mn(1)–O(3)#4	87.37(17)	O(7)#3–Mn(1)–O(3)#5	92.63(17)
O(7)–Mn(1)–O(1)	90.47(15)	O(7)#3–Mn(1)–O(1)	89.53(15)
O(3)#4–Mn(1)–O(1)	85.29(15)	O(3)#5–Mn(1)–O(1)	94.71(15)
O(7)–Mn(1)–O(1)#3	89.53(15)	O(7)#3–Mn(1)–O(1)#3	90.47(15)
O(3)#4–Mn(1)–O(1)#3	94.71(15)	O(3)#5–Mn(1)–O(1)#3	85.29(15)
O(4)#4–Mn(2)–O(11)	96.30(18)	O(4)#4–Mn(2)–O(5)#6	104.95(17)
O(11)–Mn(2)–O(5)#6	91.76(17)	O(4)#4–Mn(2)–O(2)	159.25(17)
O(11)–Mn(2)–O(2)	86.95(17)	O(5)#6–Mn(2)–O(2)	95.40(16)
2			
Mn(1)–O(1)	2.109(4)	Mn(1)–N(1)	2.242(5)
Mn(1)–O(6)#2	2.341(4)	Mn(2)#3–O(2)	2.060(4)
Mn(2)–O(3)	2.054(4)	Mn(2)#4–O(5)	2.230(4)
Mn(2)#4–O(6)	2.325(4)	Mn(2)#6–N(2)	2.185(5)
O(1)#1–Mn(1)–N(1)	93.91(16)	O(1)–Mn(1)–N(1)	86.09(16)
O(1)#1–Mn(1)–O(6)#2	93.50(15)	O(1)–Mn(1)–O(6)#2	86.50(15)
N(1)–Mn(1)–O(6)#2	94.20(17)	N(1)#1–Mn(1)–O(6)#2	85.80(17)
Mn(2)#4–O(6)–Mn(1)#5	110.10(16)	O(3)–Mn(2)–O(2)#7	103.38(18)

O(3)–Mn(2)–N(2)#8	99.49(18)	O(2)#7–Mn(2)–N(2)#8	99.68(18)
O(3)–Mn(2)–O(5)#9	97.57(19)	O(2)#7–Mn(2)–O(5)#9	157.14(17)
N(2)#8–Mn(2)–O(5)#9	85.63(18)	O(3)–Mn(2)–O(6)#9	129.66(17)
O(2)#7–Mn(2)–O(6)#9	101.43(15)	N(2)#8–Mn(2)–O(6)#9	118.51(17)
O(5)#9–Mn(2)–O(6)#9	57.30(15)		

*Symmetry modes: **1:** #1 x + 2, y, z – 1, #2 x + 1, y + 1, z, #3 –x – 2, –y – 1, –z + 2, #4 x – 2, y, z + 1, #5 –x, –y – 1, –z + 1, #6 x – 1, y – 1, z; **2:** #1 –x – 1, –y + 1, –z + 1, #2 x – 2, y, z + 1, #3 x – 1, y + 1, z + 1, #4 x + 1, y + 1, z, #5 x + 2, y, z – 1, #6 x, y, z + 1, #7 x + 1, y – 1, z – 1, #8 x, y, z – 1, #9 x – 1, y – 1, z.

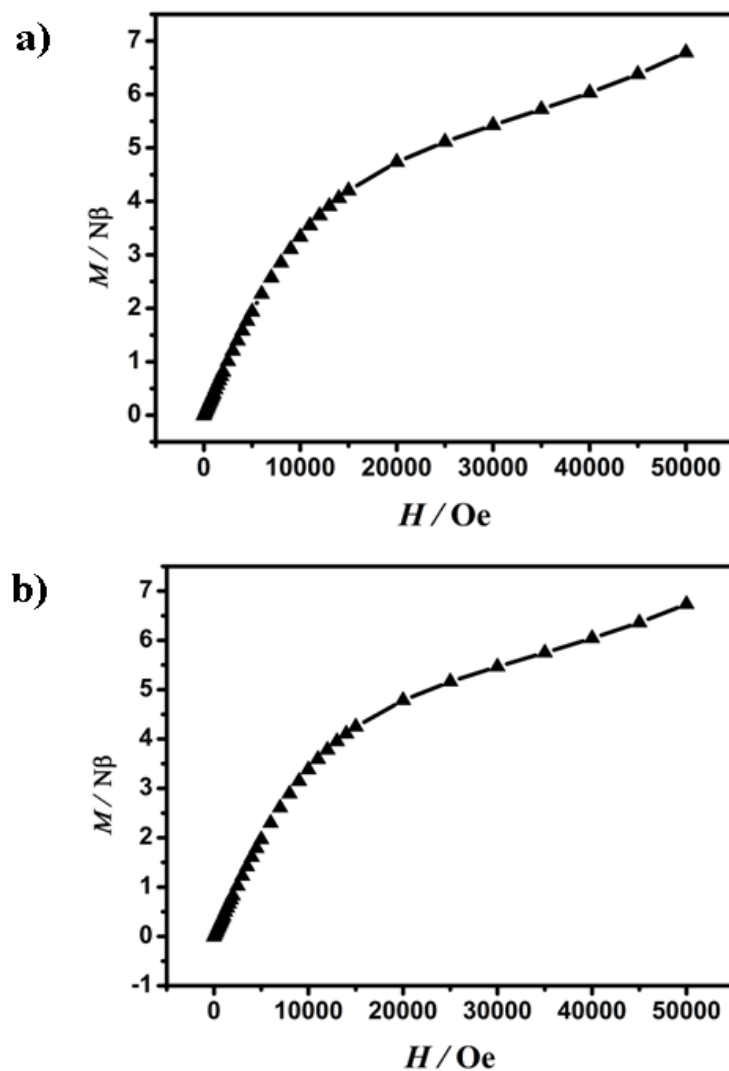


Figure S1. The M vs. H plots for **1** (a) and **2** (b) measured at 2 K.

The isotropic Heisenberg spin Hamiltonian:

$$\chi_M T = \frac{Ng^2\beta^2}{3k} \frac{\sum_{S_B, S_T} S_T(S_T+1)(2S_T+1) \exp[-\frac{E(S_B, S_T)}{kT}]}{\sum_{S_B, S_T} (2S_T+1) \exp[-\frac{E(S_B, S_T)}{kT}]} = \frac{Ng^2\beta^2}{k}$$

$$\frac{8.75 + 2.5 \exp(-5x) + 21 \exp(-7x) + 9 \exp(-10x) + 2.5 \exp(-13x) + 41.5 \exp(-16x) + 21 \exp(-17x) + 8.75 \exp(-18x) + 2.5 \exp(-19x)}{3 + 2 \exp(-5x) + 4 \exp(-7x) + 4 \exp(-10x) + 2 \exp(-13x) + 6 \exp(-16x) + 4 \exp(-17x) + 3 \exp(-18x) + 2 \exp(-19x)}$$
$$\frac{2.5 \exp(-23x) + 8.75 \exp(-24x) + 21 \exp(-25x) + 41.25 \exp(-26x) + 71.5 \exp(-27x) + 8.75 \exp(-28x) + 8.75 \exp(-30x)}{2 \exp(-23x) + 3 \exp(-24x) + 4 \exp(-25x) + 5 \exp(-26x) + 6 \exp(-27x) + 3 \exp(-28x) + 3 \exp(-30x)}$$
$$\frac{21 \exp(-31x) + 41.25 \exp(-34x) + 21 \exp(-35x) + 71.5 \exp(-37x) + 155 \exp(-40x) + 71.5 \exp(-45x) + 113.75 \exp(-50x) + 170 \exp(-55x)}{4 \exp(-31x) + 5 \exp(-34x) + 4 \exp(-35x) + 6 \exp(-37x) + 12 \exp(-40x) + 6 \exp(-45x) + 7 \exp(-50x) + 8 \exp(-55x)}$$

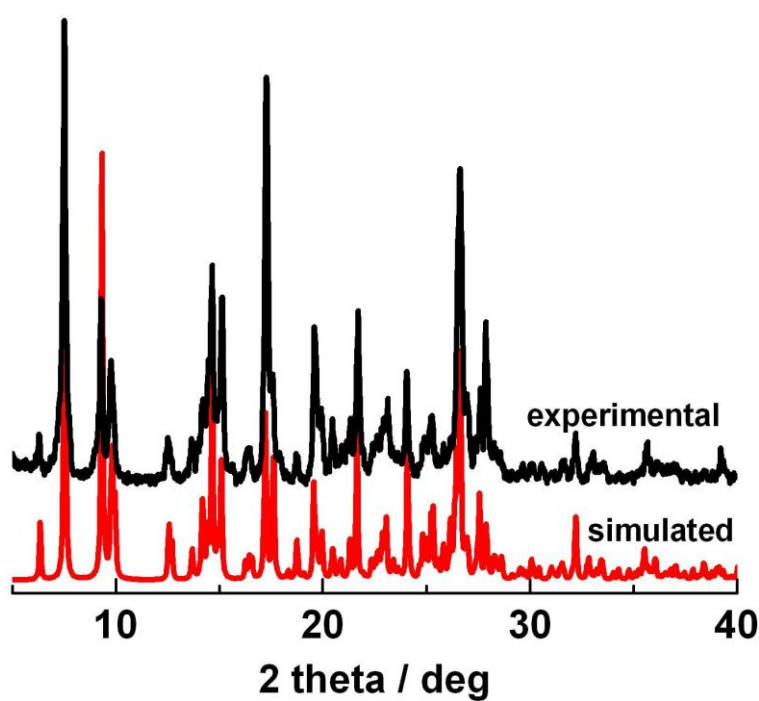


Figure S2. The simulative (red line) and experimental (black line) powder X-ray diffraction pattern for complex **1**.

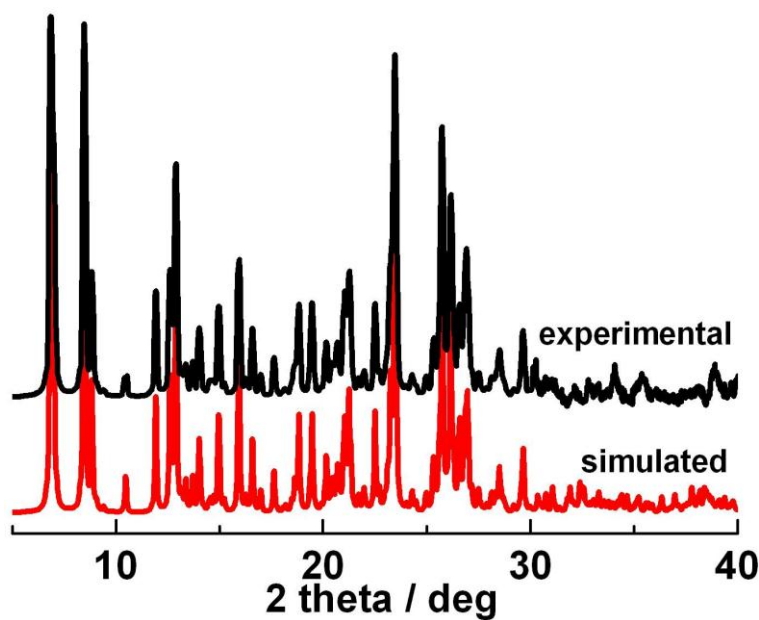


Figure S3. The simulative (red line) and experimental (black line) powder X-ray diffraction pattern for complex **2**.

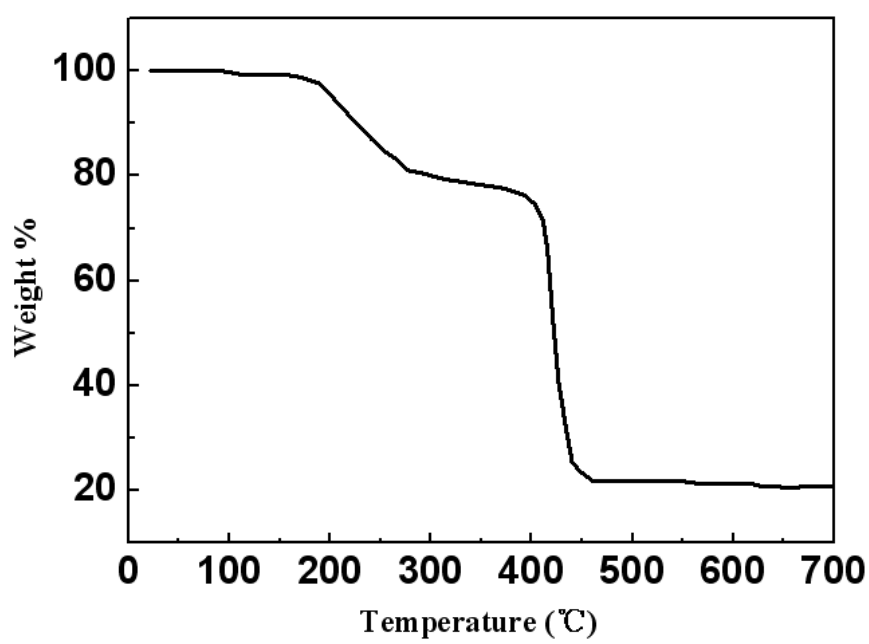


Figure S4. The TG curve of complex 1.

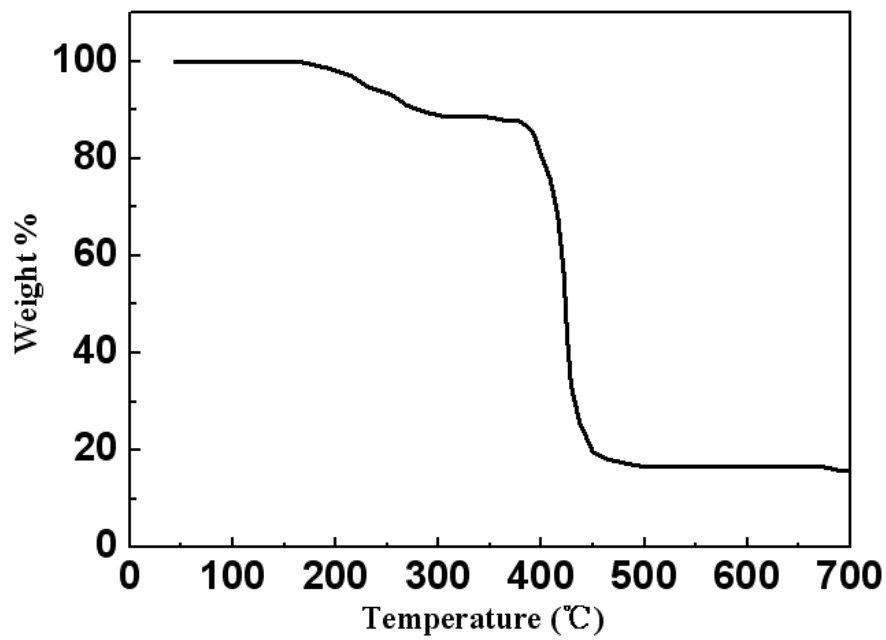


Figure S5. The TG curve of complex 2.